

Anomalies in B -decays and $U(2)$ flavour symmetry

Riccardo Barbieri^{a,d}, Gino Isidori^{b,c}, Andrea Pattori^{b,e}, Fabrizio Senia^d

(a) *Institute of Theoretical Studies, ETH Zürich, CH-8092 Zürich, Switzerland*

(b) *Physik-Institut, Universität Zürich, CH-8057 Zürich, Switzerland*

(c) *INFN, Laboratori Nazionali di Frascati, I-00044 Frascati, Italy*

(d) *Scuola Normale Superiore and INFN, Piazza dei Cavalieri 7, 56126 Pisa, Italy*

(e) *Dipartimento di Fisica e Astronomia ‘G. Galilei’, Università di Padova, Via Marzolo 8, I-35131 Padua, Italy*

Abstract

The collection of a few anomalies in semileptonic B -decays invites to speculate about the emergence of some strikingly new phenomena. Here we offer a possible interpretation of these anomalies in the context of a weakly broken $U(2)^5$ flavour symmetry and lepto-quark mediators.

1 Introduction

In the last years quite a few anomalies in semileptonic B-decays have emerged. While individually any of them requires confirmation before being taken under serious consideration, their collection motivates to speculate about the possible emergence of some strikingly new phenomena. The purpose of this paper is to offer a possible interpretation of these anomalies in the context of a weakly broken $U(2)^n$ -flavour symmetry.

The observations we refer to have received and are receiving a lot of attention. The deviations from the SM that are both statistically more significant and whose theoretical error is negligible (compared to the present experimental error) can be summarized as follows:

- An overall 3.9σ deviation from τ/l universality ($l = \mu, e$) in charged current semileptonic $B \rightarrow D^{(*)}$ decays [1–3]:¹

$$R_{D^{(*)}}^{\tau/l} = \frac{\mathcal{B}(\bar{B} \rightarrow D^{(*)}\tau\bar{\nu})/\mathcal{B}(\bar{B} \rightarrow D^{(*)}\tau\bar{\nu})_{SM}}{\mathcal{B}(\bar{B} \rightarrow D^{(*)}l\bar{\nu})/\mathcal{B}(\bar{B} \rightarrow D^{(*)}l\bar{\nu})_{SM}}, \quad (1.1)$$

$$R_D^{\tau/l} = 1.37 \pm 0.17, \quad R_{D^*}^{\tau/l} = 1.28 \pm 0.08 \quad (1.2)$$

- A 2.6σ deviation from μ/e universality in the neutral current $b \rightarrow s$ transition [4]:

$$R_K^{\mu/e} = \frac{\mathcal{B}(B \rightarrow K\mu^+\mu^-)}{\mathcal{B}(B \rightarrow Ke^+e^-)} = 0.745_{-0.074}^{+0.090} \pm 0.036 \quad (1.3)$$

predicted to be one in the Standard Model (SM) with better than 1% accuracy.

This last neutral current anomaly may be related to other tensions with the SM in the branching ratios and in the angular distributions of semileptonic $b \rightarrow s$ transitions, particularly in $B \rightarrow K^{(*)}\mu^+\mu^-$ and $B \rightarrow \phi\mu^+\mu^-$ (see Ref. [7, 8] for an updated discussion).

The interpretation of a 30% deviation from the SM in a tree level charged current interaction, eq. (1.2), calls for an exchange capable to produce at low energy an effective 4-fermion interaction proportional to the operator $(\bar{c}_L\gamma_\mu b_L)(\bar{\tau}_L\gamma_\mu\nu_L)$. On these grounds one may want to interpret the neutral current anomaly in eq. (1.3) as also due to an LL operator of the form $(\bar{s}_L\gamma_\mu b_L)(\bar{\mu}_L\gamma_\mu\mu_L)$. Although not exclusively, it is known that such an operator can as well improve the fit in the angular distribution of the semileptonic $b \rightarrow s$ transitions [7, 8]. There is however a problem to face. While both anomalies hint at a $20 \div 30\%$ deviation from the SM, there is an important difference among them. The charged current anomaly is a deviation from a SM tree level amplitude involving the third generation of leptons, whereas the neutral current one is a putative correction to a SM loop effect only concerning the first two generations of leptons.

This motivates us to ask whether there is a flavour group \mathcal{G}_F and a tree level exchange Φ such that:

- With unbroken \mathcal{G}_F , Φ couples to the third generation of quarks and leptons only;

¹ The results in eq. (1.2) are obtained using the theory predictions $\mathcal{B}(B \rightarrow D^*\tau\nu)/\mathcal{B}(B \rightarrow D^*\ell\nu)_{SM} = 0.252 \pm 0.003$ [5] and $\mathcal{B}(B \rightarrow D\tau\nu)/\mathcal{B}(B \rightarrow D\ell\nu)_{SM} = 0.300 \pm 0.008$ [6].

- After \mathcal{G}_F -breaking, the needed operators, as mentioned in the previous paragraph, are generated as a small perturbation.

The answer is positive with

$$\mathcal{G}_F = \mathcal{G}_F^q \times \mathcal{G}_F^l \quad (1.4)$$

$$\mathcal{G}_F^q = U(2)_Q \times U(2)_u \times U(2)_d \times U(1)_{d3}, \quad \mathcal{G}_F^l = U(2)_L \times U(2)_e \times U(1)_{e3}, \quad (1.5)$$

in the notation of Ref. [9, 10], and Φ is a leptoquark singlet under \mathcal{G}_F , carrying either one of the following quantum numbers under the SM gauge group:

1. $U_\mu = (3, 1)_{2/3}$, Vector singlet-model;
2. $\mathcal{U}_\mu = (3, 3)_{2/3}$, Vector triplet-model;
3. $S = (\bar{3}, 3)_{1/3}$, Scalar triplet-model.

Dynamical explanations of the above anomalies have already been proposed in the literature both in terms of vector uncoloured mediators [11] and in terms of leptoquark mediators [12–14].² Here we focus on the specific realization of leptoquark models based on the flavor group \mathcal{G}_F since:

- i) this explains their dominant coupling to the third generation only (in particular only to the left-handed quark and lepton doublets which are the only \mathcal{G}_F -invariant fermions);
- ii.) the breaking of \mathcal{G}_F specifies the source of the flavour violating couplings needed to give rise predominantly to the operator $(\bar{c}_L \gamma_\mu b_L)(\bar{\tau}_L \gamma_\mu \nu_L)$ and, at a weaker level, to $(\bar{s}_L \gamma_\mu b_L)(\bar{\mu}_L \gamma_\mu \mu_L)$ as well.

About the needed breakings of \mathcal{G}_F , we stick to the minimal set of spurions

$$y_{d3} = (1, 1, 1)_{-1} \quad \Delta_u = (2, \bar{2}, 1)_0 \quad \Delta_d = (2, 1, \bar{2})_0 \quad \mathbf{V}_Q = (2, 1, 1)_0 \quad (1.6)$$

for \mathcal{G}_F^q [9] and

$$y_{e3} = (1, 1)_{-1} \quad \Delta_e = (2, \bar{2})_0 \quad \mathbf{V}_L = (2, 1)_0 \quad (1.7)$$

for \mathcal{G}_F^l [17, 18].

In the following we write down in the three cases above the leptoquark (LQ) couplings to the fermions in their physical bases after inclusion of \mathcal{G}_F -breaking (Section 2) and we calculate the relevant amplitudes at tree level (Section 3). Consistency with current data is achieved only by the $U_\mu = (3, 1)_{2/3}$ model above. The dominant loop effects when the tree level amplitude vanishes are calculated in Section 4 for the surviving vector-singlet model. The overall consistency of the model with data is illustrated in Section 5, where further expected signals are also examined. A tentative UV completion of the phenomenological model is briefly outlined in Section 6. Summary and conclusions are drawn in Section 7.

² Leptoquark explanations of a single set of anomalies (either neutral or charged currents) have been discussed in Ref. [15]. For a recent discussion of the two set of anomalies in terms of effective four-fermion operators see Ref. [16].

2 Leptoquark Lagrangians after \mathcal{G}_F -symmetry breaking

The couplings of the three LQ to the SM electroweak doublets Q_L and L_L are (a is an index in the vector representation of $SU(2)_L$, whereas the colour indices are left understood)

$$\mathcal{L}_1 = g_U(\bar{Q}_L \gamma^\mu F L_L) U_\mu + \text{h.c} \quad (2.1)$$

$$\mathcal{L}_2 = g_{\vec{U}}(\bar{Q}_L \gamma^\mu \frac{\sigma^a}{2} F L_L) U_\mu^a + \text{h.c} \quad (2.2)$$

$$\mathcal{L}_3 = g_{\vec{S}}(\bar{Q}_L^c \frac{\sigma^a}{2} F(i\sigma^2 L_L)) S^a + \text{h.c}; \quad Q_L^c \equiv (Q_L)^c \quad (2.3)$$

where F is a matrix in flavour space which, in the \mathcal{G}_F symmetric limit, is $F_{ij} = \delta_{i3}\delta_{j3}$. On the other hand, after symmetry breaking along the directions (1.6) and (1.7), F takes the form

$$F_{ij} = \delta_{i3}\delta_{j3} + aV_{Q_i}\delta_{j3} + b\delta_{i3}V_{L_j} + cV_{Q_i}V_{L_j} \quad (2.4)$$

where, by symmetry transformations, we can write

$$V_Q = \begin{pmatrix} 0 \\ \epsilon_Q \\ 0 \end{pmatrix} \quad V_L = \begin{pmatrix} 0 \\ \epsilon_l \\ 0 \end{pmatrix} \quad (2.5)$$

in terms of two small real parameters ϵ_Q, ϵ_L and a, b, c are arbitrary coefficients, generically of order unity, that we shall also take real for simplicity. In eq. (2.4) we are neglecting terms proportional to the product $y_b y_\tau$ of the bottom and τ Yukawa couplings or to products of $\Delta_{u,d,e}$. At the same time and in the same bases as eq. (2.4), the Yukawa matrices for the charged fermions take the form

$$Y_u = \left(\begin{array}{c|c} \Delta_u & y_t \mathbf{V}_Q \\ \hline 0 & y_t \end{array} \right) \quad Y_d = \left(\begin{array}{c|c} \Delta_d & y_b x_b \mathbf{V}_Q \\ \hline 0 & y_b \end{array} \right) \quad Y_e = \left(\begin{array}{c|c} \Delta_e & y_\tau \mathbf{V}_L \\ \hline 0 & y_\tau \end{array} \right)$$

where x_b is another unknown coefficient in general of order unity.

One goes to the physical bases for all the charged fermions by an approximate diagonalization of these Yukawa matrices. In these physical bases the LQ interaction Lagrangians acquire the form

$$\mathcal{L}_1 = g_U(\bar{u}_L \gamma^\mu F^U \nu_L + \bar{d}_L \gamma^\mu F^D e_L) U_\mu + \text{h.c} \quad (2.6)$$

$$\mathcal{L}_2 = \frac{g_{\vec{U}}}{\sqrt{2}} \left[\frac{1}{\sqrt{2}} (\bar{u}_L \gamma^\mu F^U \nu_L - \bar{d}_L \gamma^\mu F^D e_L) U_\mu^{2/3} + (\bar{u}_L \gamma^\mu F^U e_L) U_\mu^{5/3} + (\bar{d}_L \gamma^\mu F^D \nu_L) U_\mu^{-1/3} \right] + \text{h.c} \quad (2.7)$$

$$\mathcal{L}_3 = \frac{g_{\vec{S}}}{\sqrt{2}} \left[\frac{1}{\sqrt{2}} (\bar{u}_L^c F^U e_L + \bar{d}_L^c F^D \nu_L) S^{1/3} + (\bar{u}_L^c F^U \nu_L) S^{-2/3} + (\bar{d}_L^c F^D e_L) S^{4/3} \right] + \text{h.c} \quad (2.8)$$

where

$$F^U = \begin{pmatrix} V_{ub}(s_l \epsilon_l) A_u & V_{ub}(c_l \epsilon_l) A_u & V_{ub}(1-a)r_u \\ V_{cb}(s_l \epsilon_l) A_u & V_{cb}(c_l \epsilon_l) A_u & V_{cb}(1-a)r_u \\ V_{tb}(s_l \epsilon_l)(b-1) & V_{tb}(c_l \epsilon_l)(b-1) & V_{tb} \end{pmatrix} \quad (2.9)$$

$$F^D = \begin{pmatrix} V_{td}(s_l \epsilon_l) A_d & V_{td}(c_l \epsilon_l) A_d & V_{td}[1-(1-a)r_u] \\ V_{ts}(s_l \epsilon_l) A_d & V_{ts}(c_l \epsilon_l) A_d & V_{ts}[1-(1-a)r_u] \\ V_{tb}(s_l \epsilon_l)(b-1) & V_{tb}(c_l \epsilon_l)(b-1) & V_{tb} \end{pmatrix} \quad (2.10)$$

$$r_u = \frac{1}{1 - x_b} \quad A_u = r_u(b - 1 + a - c) \quad A_d = b - 1 - A_u \quad (2.11)$$

and θ_l is the angle ($s_l = \sin \theta_l$, $c_l = \cos \theta_l$) in the unitary transformation that diagonalizes Δ_l on the left side. We are working in the basis of neutrino current-eigenstates, where the charged current leptonic weak interactions are flavour-diagonal. We are also neglecting a phase in the $1 - 3, 3 - 1$ elements of these flavour matrices since it does not play any role in our following considerations.

3 Tree-level amplitudes

In the three models defined in Section 1 the tree-level exchanges of the corresponding LQ give rise to effective Lagrangians relevant to charged-current and neutral-current semileptonic B and K decays. For $b \rightarrow c\tau\bar{\nu}_3$ one has

$$\mathcal{L}_{eff}^{b \rightarrow c\tau\nu} = \left(-\frac{g_U^2}{M_U^2}, \frac{g_{\bar{U}}^2}{4M_{\bar{U}}^2}, \frac{g_S^2}{8M_S^2}\right) r_u V_{cb} (1 - a) (\bar{c}_L \gamma_\mu b_L) (\bar{\tau}_L \gamma_\mu \nu_{3L}) \quad (3.1)$$

to be compared with the SM result

$$\mathcal{L}_{SM}^{b \rightarrow c\tau\nu} = -\frac{g^2}{2M_W^2} V_{cb} (\bar{c}_L \gamma_\mu b_L) (\bar{\tau}_L \gamma_\mu \nu_{3L}). \quad (3.2)$$

In both cases (SM and LQ exchange) the $b \rightarrow u\tau\bar{\nu}_3$ effective Lagrangians are obtained from the above ones with the exchange $c \rightarrow u$ and $V_{cb} \rightarrow V_{ub}$.

For the neutral-current processes $b \rightarrow s\ell\bar{\ell}$, with $\ell = e, \mu, \tau$, the LQ exchange gives

$$\begin{aligned} \mathcal{L}_{eff}^{b \rightarrow s\mu\mu} = & \left(-\frac{g_U^2}{M_U^2}, -\frac{g_{\bar{U}}^2}{4M_{\bar{U}}^2}, \frac{g_S^2}{4M_S^2}\right) V_{tb} V_{ts}^* (\bar{s}_L \gamma_\mu b_L) \left[(1 - (1 - a)r_u) (\bar{\tau}_L \gamma_\mu \tau_L) \right. \\ & \left. + (c_l \epsilon_l)^2 (b - 1) A_d (\bar{\mu}_L \gamma_\mu \mu_L) + (s_l \epsilon_l)^2 (b - 1) A_d (\bar{e}_L \gamma_\mu e_L) \right], \end{aligned} \quad (3.3)$$

whereas the lepton-universal local $b \rightarrow s\ell\bar{\ell}$ effective interaction present in the SM reads

$$\mathcal{L}_{SM}^{b \rightarrow s\ell\ell} \approx -\frac{8G_F}{\sqrt{2}} V_{tb} V_{ts}^* \frac{\alpha}{4\pi} C_9^{SM} (\bar{s}_L \gamma_\mu b_L) (\bar{\ell}_L \gamma_\mu \ell_L), \quad (3.4)$$

with $C_9^{SM} \approx 4.2$. Finally, for $b \rightarrow s\nu_3\bar{\nu}_3$ and $s \rightarrow d\nu_3\bar{\nu}_3$ amplitudes, the LQ exchange gives

$$\begin{aligned} \mathcal{L}_{eff}^{b(s) \rightarrow s(d)\nu\nu} = & \left(0, -\frac{g_{\bar{U}}^2}{2M_{\bar{U}}^2}, \frac{g_S^2}{8M_S^2}\right) (\bar{\nu}_{3L} \gamma_\mu \nu_{3L}) \left[V_{tb} V_{ts}^* ((1 + r_u(a - 1)) (\bar{s}_L \gamma_\mu b_L) \right. \\ & \left. + V_{ts} V_{td}^* |1 + r_u(a - 1)|^2 (\bar{d}_L \gamma_\mu s_L) \right], \end{aligned} \quad (3.5)$$

to be compared with

$$\mathcal{L}_{SM}^{b(s) \rightarrow s(d)\nu\nu} = -\frac{8G_F}{\sqrt{2}} C_\nu^{SM} \frac{\alpha}{4\pi} \left[V_{tb} V_{ts}^* (\bar{s}_L \gamma_\mu b_L) + V_{ts} V_{td}^* (\bar{d}_L \gamma_\mu s_L) \right] \sum_{i=1}^3 (\bar{\nu}_{iL} \gamma_\mu \nu_{iL}), \quad (3.6)$$

where $C_\nu^{SM} \approx -6.3$ (and we have omitted the sub-leading charm contribution in the $s \rightarrow d\nu\bar{\nu}$ case). Note the absence of a tree level contribution to $b \rightarrow s\nu\bar{\nu}$ from the $SU(2)$ -singlet vector LQ (model 1), as noted first in Ref. [12].

3.1 Tree-level constraints on the parameter spaces

From eq.s (3.1,3.2), neglecting small corrections to $\mathcal{B}(\bar{B} \rightarrow D^{(*)}l\bar{\nu})$ suppressed by the ϵ_l factor, one has for the three models of Section 1

$$R_{D^{(*)}}^{\tau/l} \approx 1 + (R_U, -\frac{1}{4}R_{\bar{U}}, -\frac{1}{8}R_{\bar{S}})r_u(1-a) \quad (3.7)$$

where

$$(R_U, R_{\bar{U}}, R_{\bar{S}}) = \frac{4M_W^2}{g^2} \left(\frac{g_U^2}{M_U^2}, \frac{g_{\bar{U}}^2}{M_{\bar{U}}^2}, \frac{g_{\bar{S}}^2}{M_{\bar{S}}^2} \right). \quad (3.8)$$

Similarly from eq.s (3.5, 3.6) one has

$$R_{K^{(*)}\nu} = \frac{\mathcal{B}(\bar{B} \rightarrow K^{(*)}\nu\bar{\nu})}{\mathcal{B}(\bar{B} \rightarrow K^{(*)}\nu\bar{\nu})_{SM}} \approx \frac{1}{3} \left(3 + 2\text{Re}(x) + |x|^2 \right) \quad (3.9)$$

where for the various models it is

$$(x_U, x_{\bar{U}}, x_{\bar{S}}) = -\frac{\pi}{\alpha C_{\nu}^{SM}} [1 - r_u(1-a)] \left(0, -\frac{R_{\bar{U}}}{2}, \frac{R_{\bar{S}}}{8} \right). \quad (3.10)$$

A similar formula holds also for $R_{\pi\nu\bar{\nu}} = \mathcal{B}(K \rightarrow \pi\nu\bar{\nu})/\mathcal{B}(K \rightarrow \pi\nu\bar{\nu})_{SM}$, in the limit where we neglect the subleading charm contribution and replace $[1 - r_u(1-a)]$ with $[1 - r_u(1-a)]^2$.

Unlike the case for $\mathcal{L}_{eff}^{b \rightarrow s\mu\mu}$, both $R_{D^{(*)}}^{\tau/l}$ and $R_{K^{(*)}\nu}$ depend on a single combination of flavour parameters $\beta = 1 - r_u(1-a)$. This puts a strong constraint on models 2 and 3 of Section 1, shown in Fig. 1 (for $R_{K^{(*)}\nu}$ we use the bound $R_{K^{(*)}\nu} < 4.3$ [19]), making them highly disfavoured [12]. From now on we therefore concentrate our attention on model 1 with a Vector-singlet LQ.

For later use, $R_K^{\mu/e}$ in this model is

$$R_K^{\mu/e} = \frac{\mathcal{B}(B \rightarrow K\mu^+\mu^-)}{\mathcal{B}(B \rightarrow Ke^+e^-)} = 1 + \left(\frac{2\pi}{\alpha C_9^{SM}} \right) [(b-1)A_d] R_U \epsilon_l^2 (1 - 2s_l^2), \quad (3.11)$$

while the corresponding τ/e and τ/μ ratios are

$$R_K^{\tau/e} \approx R_K^{\tau/\mu} \approx \left| 1 + \left(\frac{\pi}{\alpha C_9^{SM}} \right) [1 - (1-a)r_u] R_U \right|^2 \approx 10^2 \times |1 - (1-a)r_u|^2 \times \left(\frac{R_U}{0.1} \right)^2. \quad (3.12)$$

The result in eq. (3.12) holds for any $b \rightarrow s\tau\bar{\tau}$ rate, e.g. also for $\mathcal{B}(B \rightarrow \tau^+\tau^-)$ and $\mathcal{B}(B \rightarrow K^*\tau^+\tau^-)$, normalized to its corresponding SM value. At present this does not represent a significant constraint given that the experimental upper bounds on these modes are still 3 orders of magnitude above the SM level [19], but in the future this large enhancement could provide a striking low-energy signature of the model.

To conclude this section, it is worth comparing the tree-level effects induced by the LQ exchange (model 1) with those analyzed in Ref. [11] assuming a vector uncoloured mediator. The structure of the semileptonic operators generated is the same, but the relative weight of charged- and neutral-current terms is different: in Ref. [11] the neutral-current operators receive an additional overall suppression factor. This is why in Ref. [11] the non-standard effects are much smaller in the case of $b \rightarrow s\nu\bar{\nu}$ and $b \rightarrow s\tau\bar{\tau}$ transitions. Another difference is the absence, at the tree-level, of LQ contributions to B -meson mixing. However, as we will discuss next, this difference is only apparent: quadratically divergent contributions to $\Delta F = 2$ amplitudes are generated in the LQ case at the one-loop level and, similarly to the case of Ref. [11], B -meson mixing represents a significant constraint on the model.

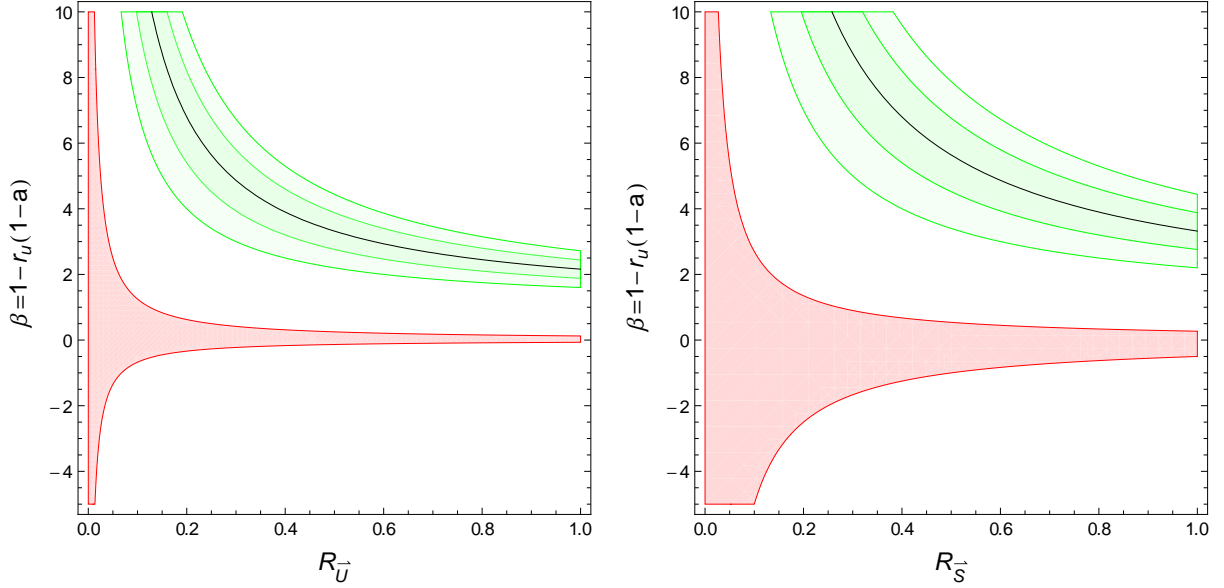


Figure 1. Allowed parameter spaces for the Vector-triplet \vec{U} (left, $R_{\vec{U}} = 4g_{\vec{U}}^2 M_W^2 / g^2 M_{\vec{U}}^2$) and for the Scalar-triplet \vec{S} (right, $R_{\vec{S}} = 4g_{\vec{S}}^2 M_W^2 / g^2 M_{\vec{S}}^2$) from $R_{D^{(*)}}^{\tau/l}$ (at 1σ (2σ) darker (lighter) green region) and $R_{K^{(*)}\nu}$ (red region).

4 Loop effects

Several processes exist which do not take place in the leptoquark models under consideration at tree level, but appear only at the one loop level. A relevant example, as already noticed, is the $b \rightarrow s\nu\bar{\nu}$ amplitude in the $SU(2)$ -singlet vector leptoquark model 1 of Section 1. Since several of these processes can give significant constraints, a one loop calculation is necessary, especially, but not only, when there are quadratically divergent contributions.

For the Lagrangian that describes the free propagation of the leptoquark U_μ and its interactions with the SM gauge bosons we take

$$\mathcal{L}_U = -\frac{1}{2}U_{\mu\nu}^\dagger U^{\mu\nu} + M_U^2 U_\mu^\dagger U_\mu + \mathcal{L}_{an} \quad (4.1)$$

where

$$U_{\mu\nu} = D_\nu U_\mu - D_\mu U_\nu \quad D_\mu \equiv \partial_\mu - ig_s \frac{\lambda^a}{2} G_\mu^a - ig' \frac{2}{3} B_\mu, \quad (4.2)$$

and

$$\mathcal{L}_{an} = -ig_s k_s (U_\mu^\dagger \frac{\lambda^a}{2} U_\nu) G^{\mu\nu a} - ig' \frac{2}{3} k_Y U_\mu^\dagger U_\nu B^{\mu\nu} \quad (4.3)$$

with obvious meaning of the symbols. \mathcal{L}_U is gauge invariant under the SM group for any value of k_s and k_Y . The overall interaction Lagrangian of the leptoquark with the B_μ field is therefore

$$\mathcal{L}_{UUB} = ig' \frac{2}{3} \left[(\partial_\alpha U_\beta^\dagger - \partial_\beta U_\alpha^\dagger) B^\alpha U^\beta - (\partial_\alpha U_\beta - \partial_\beta U_\alpha) B^\alpha U^{\beta\dagger} - k_Y U_\mu^\dagger U_\nu \partial_\mu B_\nu + k_Y U_\mu U_\nu^\dagger \partial_\mu B_\nu \right] \quad (4.4)$$

As a non trivial check of our calculations it will be useful to notice that, for $k_Y = 1$ and $2/3g' = g$, eq. (4.4) becomes the triple vertex among the W bosons in the SM with the

identifications

$$B_\mu \rightarrow W_{3\mu}, \quad U_\mu \rightarrow W_\mu^+, \quad U_\mu^+ \rightarrow W_\mu^-. \quad (4.5)$$

for a fixed color component of the leptoquark field.

4.1 Quadratically divergent loop effects

From exchanges of the U_μ vector quadratically divergent corrections appear: i) in the 2-point function of the B_μ field; ii) in the 3-point function between B_μ and the fermion fields; iii) in box-diagram contributions to various 4-fermion interactions. Below we list the relevant corrections.

4.1.1 Two and three-point functions

In the LQ model we have the following contribution to the B_μ propagator

$$\Pi_{\mu\nu}^{BB} = ig_{\mu\nu} \left[-k_Y^2 \frac{(4/9)g'^2}{64\pi^2} \frac{q^4}{M_U^2} \frac{\Lambda^2}{M_U^2} \right] \quad (4.6)$$

We do not include a correction to $\Pi_{\mu\nu}^{BB}$ at $q^2 = 0$, which vanishes by electromagnetic gauge invariance, nor a contribution proportional to q^2 since it is reabsorbed in a redefinition of g' .

Similarly one has Λ^2 -divergences in the 3-point correlation functions with an external B_μ field

$$\mathcal{M}_{B \rightarrow L_3 \bar{L}_3} = -ik_Y \frac{(2/3)g'}{64\pi^2} g_U^2 \frac{q^2}{M_U^2} \frac{\Lambda^2}{M_U^2} (\bar{u}_{L3} \not{\epsilon} P_L v_{L3}) \quad (4.7)$$

$$\mathcal{M}_{B \rightarrow Q_3 \bar{Q}_3} = ik_Y \frac{(2/3)g'}{64\pi^2} g_U^2 \frac{q^2}{M_U^2} \frac{\Lambda^2}{M_U^2} (\bar{u}_{Q3} \not{\epsilon} P_L v_{Q3}) \quad (4.8)$$

As remarked above, this implies the presence in the SM in the unitary gauge of similar contributions in the 2 and 3-point functions of the W_μ^a field, at $g' = 0$,

$$\Pi_{\mu\nu}^{ab} = ig_{\mu\nu} \delta^{ab} \left[-\frac{g^2}{64\pi^2} \frac{q^4}{M_W^2} \frac{\Lambda^2}{M_W^2} \right] \quad (4.9)$$

and

$$\mathcal{M}_{W_a \rightarrow F \bar{F}} = ig \frac{g^2}{64\pi^2} \frac{q^2}{M_W^2} \frac{\Lambda^2}{M_W^2} (\bar{u}_F T^a \not{\epsilon} P_L v_F) \quad (4.10)$$

where $F = Q$ or L and T^a is the weak isospin. We have explicitly checked that quadratically divergent contributions to physical amplitudes vanish in this limit of the SM, as they should, with the inclusion of box diagrams as well.

4.1.2 Box diagrams

Some relevant flavour violating processes have Λ^2 -divergent contributions due to leptoquark box diagrams as well. The corresponding effective Lagrangian has the form

$$\mathcal{L} = \sum_a F_a W_a \frac{g_U^4}{64\pi^2} \frac{\Lambda^2}{M_U^4} O_a \quad (4.11)$$

with the process-dependent effective operators and the corresponding coefficients ($F_a W_a$) given in Table 1.

Process	Operator	F_a	W_a	Bounds on $F_a \times (R/0.1)$
$\tau \rightarrow 3\mu$	$(\bar{\mu}\gamma^\mu P_L \tau)(\bar{\mu}\gamma_\mu P_L \mu)$	$3(b-1)^3(c_l\epsilon_l)^3$	1	1.9×10^{-2}
$\mu \rightarrow 3e$	$(\bar{e}\gamma^\mu P_L \mu)(\bar{e}\gamma_\mu P_L e)$	$3(b-1)^4(c_l\epsilon_l)(s_l\epsilon_l)^3$	1	5.5×10^{-5}
$b \rightarrow s\nu_3\bar{\nu}_3$	$(\bar{s}\gamma^\mu P_L b)(\bar{\nu}_3\gamma_\mu P_L \nu_3)$	$[1 - (1-a)r_u]$	$V_{tb}V_{ts}^*$	$[-2.5, 1.4]$
$s \rightarrow d\nu_3\bar{\nu}_3$	$(\bar{d}\gamma^\mu P_L s)(\bar{\nu}_3\gamma_\mu P_L \nu_3)$	$[1 - (1-a)r_u]^2$	$V_{ts}V_{td}^*$	$[-1.8, 0.6]$
$b\bar{s} \rightarrow \bar{b}s$	$(\bar{s}\gamma^\mu P_L b)^2$	$[1 - (1-a)r_u]^2$	$(V_{tb}V_{ts}^*)^2$	3.0×10^{-2}

Table 1. Flavour coefficients $F_a \times W_a$ for the box diagram contributions to the different processes. In the last column are the bounds from current data for $\Lambda = 4\pi M_U/g_U$ (see Section 5.3). The experimental constraints on the various processes are taken from Ref. [19].

4.2 Dipole operators

Unlike the previous cases, the coefficients of the dipole operators are not quadratically divergent. Yet they are logarithmically divergent and yield to potentially relevant constraints given the stringent experimental bounds on $\tau \rightarrow \mu\gamma$, $\mu \rightarrow e\gamma$ and $b \rightarrow s\gamma$. The leading LQ contributions to these processes are encoded by

$$\mathcal{L} = \sum_a F_a \frac{g_U^2}{32\pi^2 M_U^2} (1 - k_Y) \text{Log}\left(\frac{\Lambda^2}{M_U^2}\right) O_a \quad (4.12)$$

where

$$\mathcal{O}_{\tau\mu\gamma} = em_\tau(\bar{\mu}_L\sigma^{\alpha\beta}\tau_R)F_{\alpha\beta}, \quad F_{\tau\mu} = (b-1)(c_l\epsilon_l), \quad (4.13)$$

$$\mathcal{O}_{\mu e\gamma} = em_\mu(\bar{e}_L\sigma^{\alpha\beta}\mu_R)F_{\alpha\beta}, \quad F_{\mu e} = (b-1)^2(c_l\epsilon_l)(s_l\epsilon_l), \quad (4.14)$$

$$\mathcal{O}_{bs\gamma} = em_b(\bar{s}_L\sigma^{\alpha\beta}b_R)F_{\alpha\beta}, \quad F_{bs} = \frac{1}{3}V_{tb}V_{ts}^*[1 - (1-a)r_u]. \quad (4.15)$$

5 Consistency with data and expected signals

5.1 ElectroWeak Precision Tests

At the one loop level in the leptoquark vector-singlet model there are no corrections to the S, T, U parameters. This is due to the fact that U_μ only couples to B_μ and not to the W_μ^a -fields. There are however corrections to the ElectroWeak Precision Tests (EWPT) due to higher dimensional operators, which are at least in principle important due to Λ^2 -divergent effects.

The most effective way to see these effects is by considering the ϵ_i -parameters, as defined in [20], and their expressions in terms of vacuum-polarization, box-diagrams and vertex corrections for $S, T, U = 0$ [21]. More specifically, in the limit where one neglects the small \mathcal{G}_F -breaking, the first two generations receive corrections only from $\Pi_{\mu\nu}^{BB} = -ig_{\mu\nu}\Pi(q^2)$:

$$\epsilon_1^{(1,2)} = -e_5 \quad \epsilon_2^{(1,2)} = -s^2 e_4 - c^2 e_5 \quad \epsilon_3^{(1,2)} = c^2 e_4 - c^2 e_5 \quad (5.1)$$

where

$$e_4^{(1,2)} = -\frac{c^2}{2} \frac{d\Pi}{dq^2}(M_Z^2) = -c^2 A, \quad e_5^{(1,2)} = s^2 \frac{M_Z^2}{2} \frac{d^2\Pi}{d(q^2)^2} = s^2 A, \quad (5.2)$$

and

$$A = k_Y^2 \frac{(4/9)g'^2}{64\pi^2} \frac{M_Z^2}{M_U^2} \frac{\Lambda^2}{M_U^2}, \quad c^2 = 1 - \sin^2 \theta_W, \quad \tan \theta_W = \frac{g'}{g} \quad (5.3)$$

To estimate A , we take $\Lambda \approx 4\pi M_U/g_U$, which gives

$$A \approx \frac{k_Y^2}{36c^2} \left(\frac{gg'}{g_U^2} \right)^2 R_U \quad (5.4)$$

Given the bounds on the deviations from the SM of the ϵ_i at the 10^{-3} level, with $R_U \approx 0.1$ and $g_U^2/(gg') \gtrsim 2 \div 3$, this is a mild constraint on k_Y .

Still without any \mathcal{G}_F -breaking, a vertex correction intervenes in Z -decays to the third generation. Specifically, from eq. (4.8), the corresponding amplitudes gets corrected as

$$\delta A_\mu(Z \rightarrow \tau^+ \tau^-) = -i \frac{\delta g}{2} (\bar{u} \gamma_\mu P_L v), \quad \delta A_\mu(Z \rightarrow b \bar{b}) = i \frac{\delta g}{6} (\bar{u} \gamma_\mu P_L v), \quad (5.5)$$

where

$$\frac{\delta g}{g} = -4 \frac{s^2}{c} k_Y \frac{g_U^2}{64\pi^2} \frac{M_Z^2}{M_U^2} \frac{\Lambda^2}{M_U^2} \quad (5.6)$$

which can be estimated as

$$\left| \frac{\delta g}{g} \right| \approx s \frac{k_Y}{4c^2} \left(\frac{gg'}{g_U^2} \right) R_U \quad (5.7)$$

Consistency with the few *per mille* measurement of $\mathcal{B}(Z \rightarrow \tau^+ \tau^-)$ and $R_U \approx 0.2$ requires

$$k_Y \lesssim 3 \times 10^{-2} \frac{g_U^2}{gg'}. \quad (5.8)$$

5.2 Box diagrams and dipole operators

Some of the box diagram contributions shown in Table 1 give extra significant constraints on the parameter space of the leptoquark vector-singlet model. Such constraints are given in the last column of the same Table 1 on the modulus of the corresponding flavour coefficients, with the exception of $b \rightarrow s \nu_3 \bar{\nu}_3$ and $s \rightarrow d \nu_3 \bar{\nu}_3$, where there is an allowed range. We neglect the contributions, when present, of quadratically divergent Penguin-like contributions proportional to k_Y .

Although the coefficients of the dipole operators in Section 4.2 are not quadratically divergent, they are significant at least in the leptonic processes. The bound on the flavour coefficient relevant to $\tau \rightarrow \mu \gamma$ (obtained in the limit $k_Y = 0$) is

$$(b-1)(c_l \epsilon_l) \log(\Lambda/M_U) \lesssim 4 \times 10^{-2} \left(\frac{0.1}{R} \right) \quad (5.9)$$

whereas the one on $\mu \rightarrow e \gamma$ is

$$(b-1)^2 (s_l c_l) \epsilon_l^2 \log(\Lambda/M_U) \lesssim 5 \times 10^{-5} \left(\frac{0.1}{R} \right) \quad (5.10)$$

5.3 Overall constraints

As apparent from Sections 3.1 and 5.2 the leptoquark effects in $R_{D^{(*)}}^{\tau/l}$ (at tree level), $R_{K^{(*)}\nu}$, $\mathcal{B}(K^+ \rightarrow \pi^+ \nu \bar{\nu})$ and $b\bar{s} \rightarrow \bar{b}s$ (al loop level) are predicted in terms of two single effective parameters, R_U and $\beta = 1 - (1 - a)r_u$, for a cutoff $\Lambda \approx 4\pi M_U/g_U$. The consistency with data of all these effects is shown in Fig. 2 for $\Lambda = 4\pi M_U/g_U$. The constraint from $\Delta B_s = 2$ dominates over the others, fixing β near zero, within about $0.1 \div 0.2$. At the same time, at 1σ level, $R_U \approx 0.25 \div 0.35$.

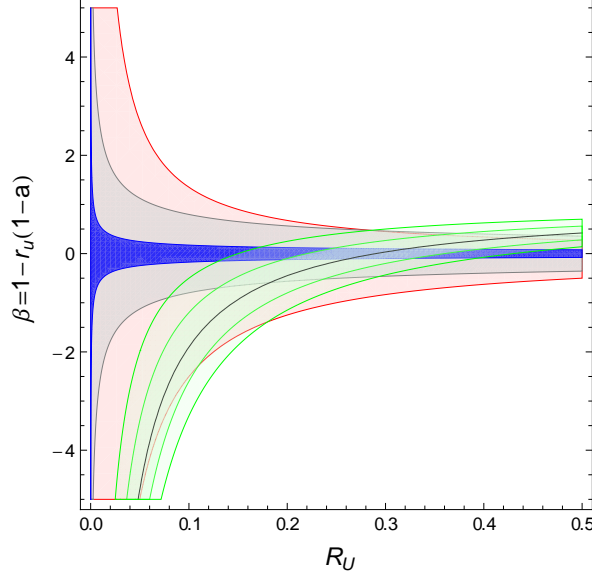


Figure 2. Allowed parameter space for the Vector-singlet U from $\Delta B_s = 2$ (blue region), $R_{D^{(*)}}^{\tau/l}$ (green), $R_{K^{(*)}\nu}$ (red) and $\mathcal{B}(K^+ \rightarrow \pi^+ \nu \bar{\nu})$ (gray). $R_U = 4g_U^2 M_W^2 / g^2 M_U^2$

The leptoquark effects in $R_K^{\mu/e}$ (at tree level) and in the purely leptonic sector (at loop level) depend, for given R_U , on ϵ_l and s_l plus two combinations of parameters, $(b - 1)$ and $A_u = r_u(b - 1 + a - c)$, generally of order unity. As shown more explicitly in a while, the dipole contribution to $\mu \rightarrow e\gamma$ in eq. (5.10) requires a small s_l . In this case the lepton flavour violating anomaly $R_K^{\mu/e}$ constrains the parameter space as shown in Fig. 3, thus setting a lower bound on the combination $[c_l \epsilon_l (b - 1)] \gtrsim 0.02$ for $A_u / (b - 1) \lesssim 5$. In turn the dipole contributions to $\tau \rightarrow \mu\gamma$ and to $\mu \rightarrow e\gamma$ (in this case for two values of s_l) are shown in Figs. 4 against the same combination of parameters and different values of Λ/M_U . Both Fig. 3 and Figs. 4 are meant to be extended symmetrically for negative values of $[c_l \epsilon_l (b - 1)]$. Note that, for not too small values of s_l , it is $\tau \rightarrow \mu\gamma$ that sets the strongest constraint. In fact, for $A_u / (b - 1) \lesssim 5$, all anomalies can be described consistently with all various constraints for values of Λ/M_U not larger than about $3 \div 4$, suggesting a strong interaction nature of the LQ.

5.4 Leptoquark pair production at LHC

The LQ production at the LHC is dominated by the QCD pair production and it depends only on M_U . A compilation of results relevant to our model 1 can be found, for instance, in

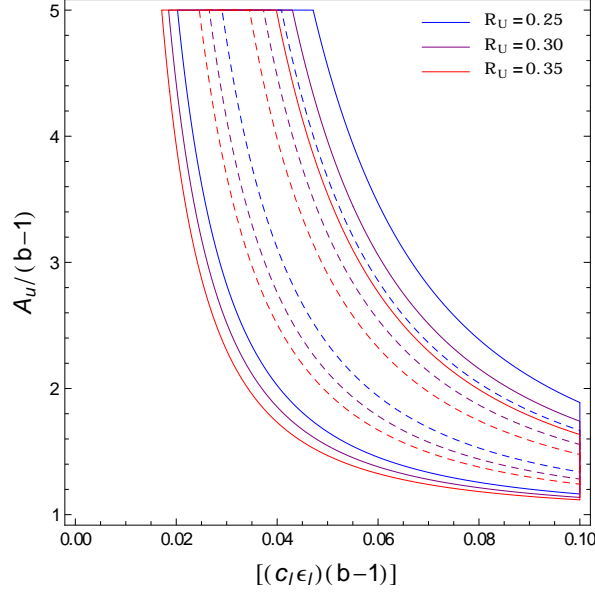


Figure 3. Allowed parameter space for the Vector-singlet U from $R_K^{\mu/e}$ for $R_U = 0.25, 0.30, 0.35$. Dotted (full) contours delimit the $1\sigma(2\sigma)$ regions.

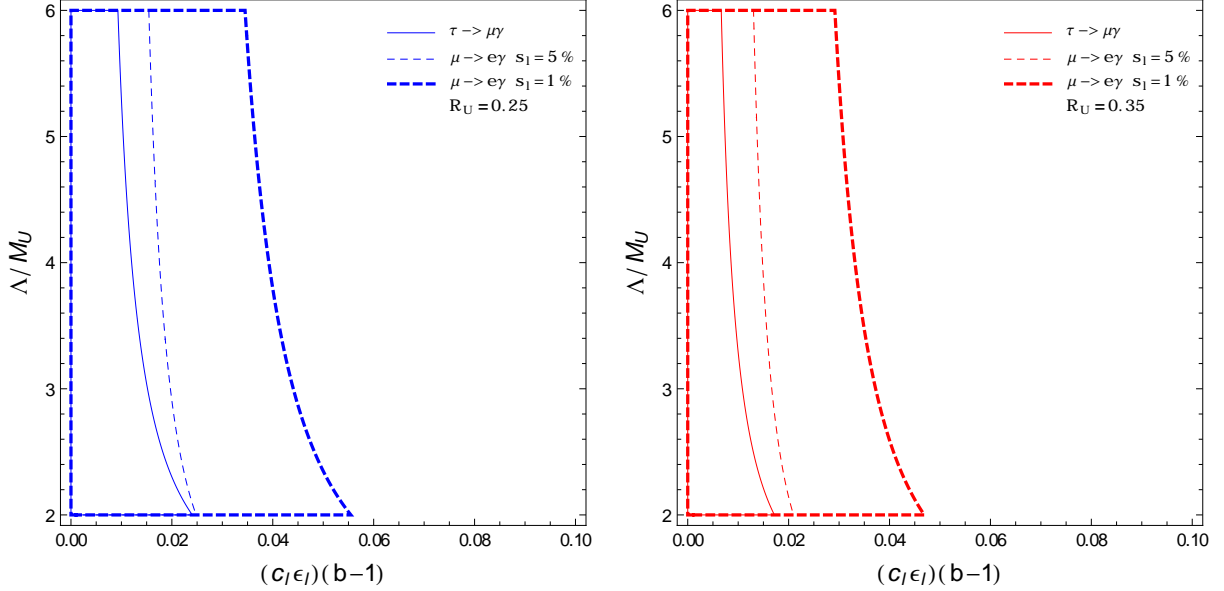


Figure 4. Allowed parameter space for the Vector-singlet U from $\tau \rightarrow \mu\gamma$ and $\mu \rightarrow e\gamma$ for $R_U = 0.25$ (left) and $R_U = 0.35$ (right).

the recent CMS analysis [22]: the cross-section varies from about 1 pb for $M_U \approx 0.5$ TeV to 3×10^{-3} pb for $M_U \approx 1.0$ TeV³.

In order to determine the LHC sensitivity to various LQ searches we need to evaluate the branching ratios in the different decay channels. At the tree-level one has

$$\Gamma(U \rightarrow q_i \ell_j) = \frac{1}{24\pi} g_U^2 |F_{ij}^{U,D}|^2 M_U \quad (5.11)$$

and, to a good accuracy, the total decay width is given by the sum of the two leading decays

³By taking $k_s = 0$ in eq. (4.3).

$(U \rightarrow t \bar{\nu}_\tau, b \bar{\tau})$: $\Gamma_{\text{tot}} = g_U^2 M_U / (12\pi)$. The branching ratios are then just given by

$$\mathcal{B}(U \rightarrow u_i \bar{\nu}_j) = \frac{1}{2} |F_{ij}^U|^2, \quad \mathcal{B}(U \rightarrow d_i \ell_j^+) = \frac{1}{2} |F_{ij}^D|^2. \quad (5.12)$$

For the searches in the second-generation channels performed in Ref. [22] ($U\bar{U} \rightarrow \mu\mu jj$ and $U\bar{U} \rightarrow \mu\nu jj$, where j denote a light-quark jet) we find

$$\begin{aligned} \mathcal{B}(U\bar{U} \rightarrow \mu\mu jj) &= \left(\frac{1}{2} \sum_{i=d,s} |F_{i2}^D|^2 \right)^2 \approx (8.5 \times 10^{-7}) \times c_l^4 \epsilon_l^4 \\ \mathcal{B}(U\bar{U} \rightarrow \mu\nu jj) &= \frac{1}{2} \sum_{i=d,s} |F_{i2}^D|^2 \times \frac{1}{2} \sum_{j=u,c} (|F_{j2}^U|^2 + |F_{j1}^U|^2) \approx (7.7 \times 10^{-7}) \times c_l^2 \epsilon_l^4, \end{aligned} \quad (5.13)$$

from which we deduce that these searches do not put any significant constraint on the model.

On the other hand, a relevant constraint is obtained by the dedicated search for the $U\bar{U} \rightarrow t\bar{t}\nu_\tau\bar{\nu}_\tau$ decay chain performed by ATLAS [23]. In our model $\mathcal{B}(U\bar{U} \rightarrow t\bar{t}\nu_\tau\bar{\nu}_\tau) = 0.25$ that implies the limit

$$M_U > 770 \text{ GeV}. \quad (5.14)$$

By a naive scaling of the statistics and the cross-section, we estimate that this limit could improve up to 1.3 TeV, in absence of a signal, with 300 fb^{-1} at 13 TeV.

Taking into account the constraints on R_U in Fig. 2, the bound on M_U can be turned into a bound on g_U . For $R_U > 0.2$ we get $g_U > 1.4$, that would raise to $g_U > 2.4$ in absence of a direct signal with 300 fb^{-1} at 13 TeV.

6 A naive composite leptoquark picture

Needless to say the phenomenological model described so far cries out for a UV completion. Here we describe an attempt in the direction of composite Higgs models, that will at least serve to illustrate the difficulties to comply with the various constraints. It does not take much to anticipate that the main such constraint comes from the value of R_U as implied by Fig. 2.

Let us consider a strongly interaction sector with a global symmetry $SU(4) \times SO(5)$ spontaneously broken down to the Pati-Salam group $SU(4) \times SU(2)_L \times SU(2)_R$, so as to generate a composite pseudo-Goldstone Higgs boson. As usual the SM group is gauged inside the residual global group. Within $SU(4)$ this structure leads to composite quasi-degenerate vectors: the composite gluons, a vector singlet carrying $B - L$ and, most importantly, the U_μ leptoquark vector.

The strong sector will also contain composite vector-like fermions in multiplets of the Pati-Salam group occurring in three flavour species. The important thing is that these composite Ψ fermions have components that match the quantum numbers of the SM fermions with respect to the SM gauge group. The requisite to make contact with the phenomenological model described in the previous Sections is that the mass mixing terms between the elementary and the composite fermions respect, up to small breaking terms, the symmetry in flavor space $U(2)_\Psi \times \mathcal{G}_F^4$. With $\Psi = (4, 2, 1) \oplus (\bar{4}, 1, 2)$ (plus complex conjugate states) it is easy

⁴If Ψ is reducible $U(2)_\Psi$ may actually be a product of $U(2)$ factors

to convince oneself that this structure shall lead, in the unbroken $U(2)_\Psi \times \mathcal{G}_F$ limit, to eq. (2.1) with

$$g_U = g^* \sin \theta_{Q3} \sin \theta_{L3} \quad (6.1)$$

and $F_{ij} = \delta_{i3}\delta_{j3}$ as the only interaction of U_μ with the standard fermions. Here g^* is the coupling of the LQ to the composite fermions and θ_{Q3}, θ_{L3} are the mixing angles of Q_3, L_3 with the same composite fermions in Ψ . Other choices of Ψ , phenomenologically motivated, shall lead to a relation between g_U and g^* involving more parameters but always respecting $g_U \leq g^*$.

The "standard" interpretation of the composite Higgs models also gives a similar mass $M \approx g^* f$ for the composite vectors in the adjoint of $SU(4)$, among which is U_μ , and f is the breaking scale of $SO(5)$ down to $SO(4)$. As a consequence the phenomenological parameter R_U becomes

$$R_U \approx \left(\frac{V}{f}\right)^2 \sin^2 \theta_{Q3} \sin^2 \theta_{L3}, \quad V = 245 \text{ GeV}, \quad (6.2)$$

independent from g^* .

7 Summary and conclusions

Being the heaviest particle in the SM, the top quark plays a special role in many processes and/or mechanisms of the greatest relevance in particle physics. It is not surprising therefore that the top quark is thought to be equally important in several BSM speculative considerations. Flavour physics is no exception to this rule. In the SM top exchanges dominate many of the observed Flavour Changing Neutral Current effects. In BSM, taking Minimal Flavour Violation as a relevant example, it is the relatively large top Yukawa coupling that controls many of the new observable phenomena that might occur.

This is the basis to consider a $U(2)^3$ approximate symmetry as a ruling symmetry of the flavor quark sector of any putative extension of the SM. More precisely $U(2)_Q \times U(2)_u \times U(2)_d \times U(1)_{d3}$, a residual symmetry of the SM with all the Yukawa coupling switched off but the top one, can allow, suitably broken, for mild deviations from the SM itself. Decays of the B mesons, in particular through the b_L -component, which is the only singlet under $U(2)^3 \times U(1)_{d3}$ other than $t_{L,R}$, are obvious candidates where such deviations might occur and be observable.

It is therefore natural to ask if and how the recently emerged anomalies in semileptonic B -decays can be accommodated in this context. As we have shown this is possible by:

- i.) invoking the exchange of a vector-singlet LQ with a relatively large value of the parameter $R_U = 4M_W^2 g_U^2 / g^2 M_U^2 \approx 0.2$, i.e. a ratio well below 1 TeV between its mass M_U and its dominant coupling g_U to the third generation of left-handed quarks and leptons;
- ii.) extending the $U(2)^3 \times U(1)_{d3}$ symmetry of the quark sector, with its breaking, to the lepton sector as well, via a $U(2)_L \times U(2)_e \times U(1)_{e3}$ flavour symmetry.

The observed anomalies arise as relatively small effects of the breaking of the overall $U(2)^5$ symmetry, thus allowing non vanishing couplings of the LQ to the lighter generations as well.

The deviation from the SM in the charged current observable $R_{D^{(*)}}^{\tau/l}$ is due to a tree level exchange of the LQ controlled, other than by R_U , by a single combination of dimensionless parameters β , as shown in Fig. 2. These same effective parameter controls the quadratically divergent one loop contributions to $B \rightarrow K\nu_3\bar{\nu}_3$, $K \rightarrow \pi\nu_3\bar{\nu}_3$ and $b\bar{s} \rightarrow \bar{b}s$, as well as the tree level effect in $b \rightarrow s\tau\bar{\tau}$. All of these processes can corroborate or exclude the LQ model by future measurements.

The lepton flavour violation emerging in the neutral current observable $R_K^{\mu/e}$ can also arise from a tree level exchange of the leptoquark, although suppressed by the intervention in the final state of muons or electrons. In this case the relevant parameters control as well the log-divergent one loop dipole moment contributions to $\tau \rightarrow \mu\gamma$ and $\mu \rightarrow e\gamma$. The current limits on both these processes are close to saturate the observed deviation of $R_K^{\mu/e}$ from unity, at least in a natural range of the relevant parameters, as illustrated in Fig. 3 and Figs 4.

To discuss the possible manifestation of the vector LQ in direct production strongly depends on being able to go beyond the low energy phenomenological picture that we have used in this paper. This is because the constraint on $R_U \approx 0.2$ only fixes the ratio M_U/g_U between the mass and the coupling of the LQ. The current LHC searches bound M_U to be bigger than about 700 GeV, independently from the value of g_U , which is therefore constrained to be bigger than about 1.4. Larger values of g_U , and therefore of M_U as well, are indirectly hinted by the constraints from $\tau \rightarrow \mu\gamma$ and $\mu \rightarrow e\gamma$. All this points towards the need of a UV completion of the phenomenological model used so far, perhaps along the lines outlined in Section 6. It will be interesting to see if and how such UV completion can be accomplished consistently with the numerous constraints.

Acknowledgments

We thank Andrea Tesi and Andrea Wulzer for useful discussions. This research was supported in part by the Swiss National Science Foundation (SNF) under contract 200021-159720.

References

- [1] J. P. Lees *et al.* [BaBar Collaboration], Phys. Rev. D **88** (2013) 7, 072012 [arXiv:1303.0571].
- [2] M. Huschle *et al.* [Belle Collaboration], Phys. Rev. D **92** (2015) 7, 072014 [arXiv:1507.03233].
- [3] R. Aaij *et al.* [LHCb Collaboration], Phys. Rev. Lett. **115** (2015) 15, 159901 [arXiv:1506.08614].
- [4] R. Aaij *et al.* [LHCb Collaboration], Phys. Rev. Lett. **113** (2014) 151601 [arXiv:1406.6482].
- [5] S. Fajfer, J. F. Kamenik and I. Nisandzic, Phys. Rev. D **85** (2012) 094025 [arXiv:1203.2654].
- [6] H. Na *et al.* [HPQCD Collaboration], Phys. Rev. D **92** (2015) 5, 054510 [arXiv:1505.03925].
- [7] S. Descotes-Genon, L. Hofer, J. Matias and J. Virto, arXiv:1510.04239.
- [8] W. Altmannshofer and D. M. Straub, Eur. Phys. J. C **75** (2015) 8, 382 [arXiv:1411.3161].
- [9] R. Barbieri, G. Isidori, J. Jones-Perez, P. Lodone and D. M. Straub, Eur. Phys. J. C **71** (2011) 1725 [arXiv:1105.2296].

- [10] R. S. Chivukula and H. Georgi, Phys. Lett. B **188** (1987) 99; L. J. Hall and L. Randall, Phys. Rev. Lett. **65** (1990) 2939; G. D’Ambrosio, G. F. Giudice, G. Isidori and A. Strumia, Nucl. Phys. B **645** (2002) 155 [hep-ph/0207036].
- [11] A. Greljo, G. Isidori and D. Marzocca, JHEP **1507** (2015) 142 [arXiv:1506.01705].
- [12] L. Calibbi, A. Crivellin and T. Ota, Phys. Rev. Lett. **115** (2015) 18, 181801 [arXiv:1506.02661].
- [13] M. Bauer and M. Neubert, arXiv:1511.01900.
- [14] S. Fajfer and N. Kosnik, arXiv:1511.06024.
- [15] A. Datta, M. Duraissamy and D. Ghosh, Phys. Rev. D **89** (2014) 7, 071501 [arXiv:1310.1937]; G. Hiller and M. Schmaltz, Phys. Rev. D **90** (2014) 054014 [arXiv:1408.1627]; B. Gripaios, M. Nardecchia and S. A. Renner, JHEP **1505** (2015) 006 [arXiv:1412.1791]; S. Sahoo and R. Mohanta, Phys. Rev. D **91** (2015) 9, 094019 [arXiv:1501.05193]; D. Becirevic, S. Fajfer and N. Kosnik, Phys. Rev. D **92** (2015) 1, 014016 [arXiv:1503.09024]; M. Freytsis, Z. Ligeti and J. T. Ruderman, Phys. Rev. D **92** (2015) 5, 054018 [arXiv:1506.08896].
- [16] B. Bhattacharya, A. Datta, D. London and S. Shivashankara, Phys. Lett. B **742** (2015) 370 [arXiv:1412.7164]; R. Alonso, B. Grinstein and J. M. Camalich, JHEP **1510** (2015) 184 [arXiv:1505.05164].
- [17] R. Barbieri, D. Buttazzo, F. Sala and D. M. Straub, JHEP **1207** (2012) 181 [arXiv:1203.4218].
- [18] G. Blankenburg, G. Isidori and J. Jones-Perez, Eur. Phys. J. C **72** (2012) 2126 [arXiv:1204.0688].
- [19] K. A. Olive *et al.* [Particle Data Group Collaboration], Chin. Phys. C **38** (2014) 090001.
- [20] G. Altarelli and R. Barbieri, Phys. Lett. B **253** (1991) 161; G. Altarelli, R. Barbieri and S. Jadach, Nucl. Phys. B **369** (1992) 3 [Nucl. Phys. B **376** (1992) 444].
- [21] R. Barbieri, M. Frigeni and F. Caravaglios, Phys. Lett. B **279** (1992) 169.
- [22] V. Khachatryan *et al.* [CMS Collaboration], arXiv:1509.03744.
- [23] G. Aad *et al.* [ATLAS Collaboration], arXiv:1508.04735.